Communication

Controlled Intercalation and Chemical Exfoliation of Layered Metal-Organic Frameworks using A Chemically Labile Intercalating Agent

Yanjun Ding, Ying-Pin Chen, Xinlei Zhang, Liang Chen, Zhaohui Dong, Hai-Long Jiang, Hangxun Xu, and Hong-Cai Zhou

J. Am. Chem. Soc., **Just Accepted Manuscript** • DOI: 10.1021/jacs.7b04829 • Publication Date (Web): 27 Jun 2017

Controlled Intercalation and Chemical Exfoliation of Layered Metal-Organic Frameworks using A Chemically Labile Intercalating Agent

Yanjun Ding,[†] Ying-Pin Chen,[‖] Xinlei Zhang,[†] Liang Chen,[†] Zhaohui Dong,[§] Hai-Long Jiang,[†,‡,*] Hangxun Xu,[†,*] and Hong-Cai Zhou[‖,*]

[†] *Department of Polymer Science and Engineering, CAS Key Laboratory of Soft Matter Chemistry, University of Science and Technology of China, Hefei, Anhui 230026, China*

[‡] *Department of Chemistry, Hefei National Laboratory for Physical Sciences at the Microscale, University of Science and Technology of China, Hefei, Anhui 230026, China*

[§] *Shanghai Synchrotron Radiation Facility, Shanghai Institute of Applied Physics, Shanghai, 201800, China*

[‖] *Department of Materials Science and Engineering, Texas A&M University, College Station, Texas 77840, United States*

Supporting Information

ABSTRACT: Creating ordered two-dimensional (2D) metal-organic framework (MOF) nanosheets has attracted extensive interest. However, it still remains a great challenge to synthesize ultrathin 2D MOF nanosheets with controlled thickness in high yields. In this work, we demonstrate a novel intercalation and chemical exfoliation approach to obtain MOF nanosheets from intrinsically layered MOF crystals. This approach involves two steps: firstly, layered porphyrin MOF crystals are intercalated with 4,4'-dipyridyl disulfide through coordination bonding with the metal nodes; subsequently, selective cleavage of the disulfide bond induces the exfoliation of intercalated MOF crystals, leading to individual, freestanding MOF nanosheets. This chemical exfoliation process can proceed efficiently at room temperature to produce ultrathin 2D MOF nanosheets (~1 nm) with ~57% overall yield. The obtained ultrathin nanosheets exhibit efficient and far superior heterogeneous photocatalysis performance to the corresponding bulk MOF.

Two-dimensional (2D) nanomaterials with atomic or molecular thickness have received broad interest in recent years due to their unique dimension-related properties and promising applications in energy storage, separation, catalysis, and nanoelectronics.[1] Recently, 2D metal-organic framework (MOF) nanosheets have emerged as a new class of 2D nanomaterials for molecular sieving, sensing, and catalysis.[2] Highly ordered ultrathin MOF nanosheets formed via coordination bonding require the precise control of structure and functionality over extended length scale. MOF nanosheets are of significant importance, not only for fundamental structure-property investigations but also for technological developments.[3] Nonetheless, the rational synthesis of MOF nanosheets with diverse structures and tailored properties while keeping them down to atomic thickness is still a great challenge.

Top-down method has been demonstrated to be a formidable approach for efficient and scalable production of various 2D nanomaterials.[4] Exfoliation of 3D layered MOFs into their 2D constituents is very attractive if appropriate exfoliation methods can be developed. For example, the layered MOFs are diverse sources of ultrathin crystalline nanosheets for molecular sieving if they can be efficiently exfoliated while retaining their structure and morphology.[2c,2d] Recent studies on exfoliation of MOFs exclusively focus on exfoliating 2D frameworks held together by interlayer van der Waals interactions or hydrogen bonding in bulk crystals.[5] Insufficient control over the mechanical or solvent mediated exfoliation process by weakening interlayer interactions in MOF crystals often leads to 2D nanosheets with various thicknesses and low yields (typically <15%).[2e,5f] To circumvent this problem, a more reliable exfoliation route using controllable chemical reactions to regulate the interlayer interactions is highly desired. Exfoliation of the chemically pre-intercalated layered inorganic solids is an efficient method to synthesize ultrathin 2D inorganic nanosheets.[6] Unfortunately, the generally used chemical intercalation method in inorganic solids is not applicable in exfoliating MOFs into 2D nanosheets.

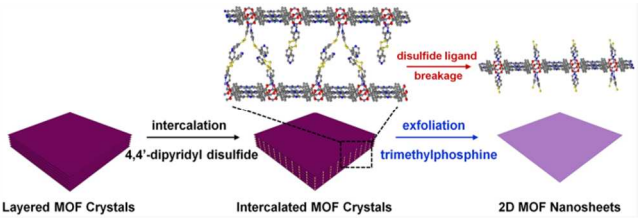

Figure 1. Schematic illustration of the overall process developed to produce 2D MOF nanosheets via an intercalation and chemical exfoliation approach.

Here, for the first time, we demonstrate a new strategy for the high-yield synthesis of 2D MOF nanosheets via chemical exfoliation from intercalated MOF crystals. The overall fabrication process is schematically illustrated in Figure 1. In order to obtain chemically responsive MOFs, we incorporate a chemically labile dipyridyl ligand, 4, 4'-dipyridyl disulfide (DPDS), into the layered MOF crystals to form new intercalated MOFs. Because the interlayer interactions are weakened between expanded 2D layers after scissoring DPDS by chemical reduction of the disulfide bond using trimethylphosphine (TMP), MOFs can be easily exfoliated into ultrathin nanosheets (~1 nm) with high yield (~57%). Furthermore, we demonstrate that the as-prepared

nanosheets exhibit very high efficiency in singlet oxygen ($^1O_2$) generation for heterogeneous photocatalysis.

Tetrakis(4-carboxyphenyl)porphyrin (TCPP) is an extensively used organic linker to construct a variety of 2D or 3D MOFs.[7] Thus, a known MOF (PPF-1) containing porphyrin sheets with Zn dinuclear paddlewheel secondary building units (SBUs) was initially used here.[8a] The 2D layers can be inserted in the third dimension by coordinating the metal centers within the paddlewheels and inside the porphyrin rings.[8] As a result, the pyridyl ligands can be inserted into the porphyrin layers to form a new crystal (Figure S1). Unfortunately, diffractions are too weak to determine the overall structure. We then tried other metallo-TCPP (M-TCPP, where M is Pd, Ni, and Co) species and obtained much better crystals by using PdTCPP (Figure S2, S3 and Table S1). Therefore, the MOF containing PdTCPP is used as model structure for this proof-of-concept study.

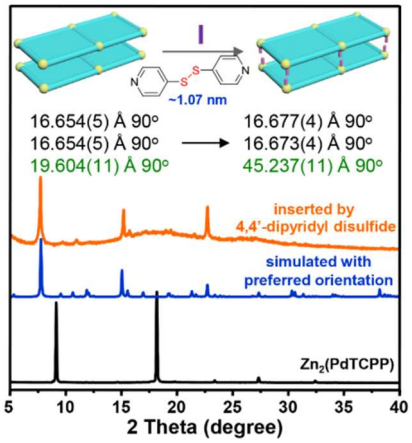

Figure 2. Experimental PXRD patterns of Zn_2(PdTCPP) before and after inserting DPDS along with simulated results considering preferred orientation in (001) direction. The unit cell parameters are obtained from single-crystal X-ray crystallography.

As shown in Figure 2, the corresponding unit cell parameter (*c*, perpendicular to porphyrin planes) increases from 19.604 to 45.237 Å after intercalation, indicating the interlayer distance varies from 9.8 to 22.6 Å which is larger than the longitudinal length of the DPDS ligand (9.3 Å). This observation indicates that only one pyridinic N from DPDS ligand coordinates Zn from $Zn_2(COO)_4$ SBU and the other is not coordinated. From the solved structure by single crystal data for the intercalated MOF, Zn_2(PdTCPP)$(DPDS)_2$ (Figure S4 and Table S1), the PdTCPP layers are clearly observed whereas the inserted DPDS linkers are incomplete because of the random orientation of the linkers caused by free rotation of single bonds.[7d] However, X-ray photoelectron spectroscopy (XPS) (Figure S5), elemental analysis, mass spectra (Figure S6) and energy-dispersive X-ray spectroscopy (Figure S7) results indicate the presence of DPDS in the crystals. Powder X-ray diffraction (PXRD) patterns further agrees that one of DPDS ligands must be coordinated the unsaturated Zn sites (Figure S8), instead of flowing in the layers. The structure is therefore confirmed by using a similar ligand, 4-(phenyldithio) pyridine (PDTP), to replace DPDS for the intercalation reaction (Figure S9). Moreover, ^{1}H NMR result of the digested MOF crystals shows a 1:2 ratio between PdTCPP and DPDS (Figure S10) which is consistent with the theoretical value. After intercalation, the MOF crystals remained the layered structure (Figure S11). Taking the preferred orientation into consideration,[2e,9] the experimental powder X-ray diffraction pattern (PXRD) coincides with the pattern simulated from the structure solved with single-crystal XRD data (Figure 2). The proposed structure describing coordinated DPDS ligands (Figure S12) was further verified using synchrotron-based powder X-ray diffraction (PXRD) pattern (Figure S13). Thus, our results indicate that DPDS can be intercalated into the layered MOF crystals to form new MOF crystals with expanded interlayer distance.[8]

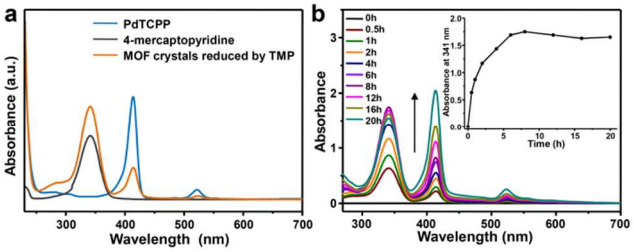

Figure 3. (a) UV-Vis absorption spectra of PdTCPP, 4-mercaptopyridine, and the intercalated MOF crystals after reduction by TMP. (b) Time course measurement of the exfoliation process by UV-vis absorption spectroscopy. Insert: the absorbance at 341 nm as a function of exfoliation time.

The disulfide intercalating reagent, DPDS, has an absorption peak at 245 nm (Figure S14). After reduction by TMP, a new peak around 341 nm corresponding to 4-mercaptopyridine appears, suggesting the DPDS is chemically scissored into 4-mercaptopyridine. Subsequently, after adding TMP into an ethanol solution containing Zn_2(PdTCPP)$(DPDS)_2$ crystals, new peaks at 341 nm and 425 nm corresponding to 4-mercaptopyridine and PdTCPP appear (Figure 3a), implying that the dipyridyl intercalating agents are cleaved (Figure S15). As shown in Figure 3b, upon adding TMP, the absorption peak at 341 nm increases and, after ~10 h, the absorption intensity reaches to the maximum value. Consequently, exfoliation of the MOF crystals into ultrathin nanosheets was carried out by adding 20-fold excess TMP into the crystal solution at room temperature with gentle stirring. Excess TMP was used to ensure that crystals were exfoliated with the highest yield. The exfoliation process occurred immediately and was evidenced by the Tyndall effect upon irradiation with a laser beam (Figure 4a). The exfoliated nanosheets were characterized by transmission

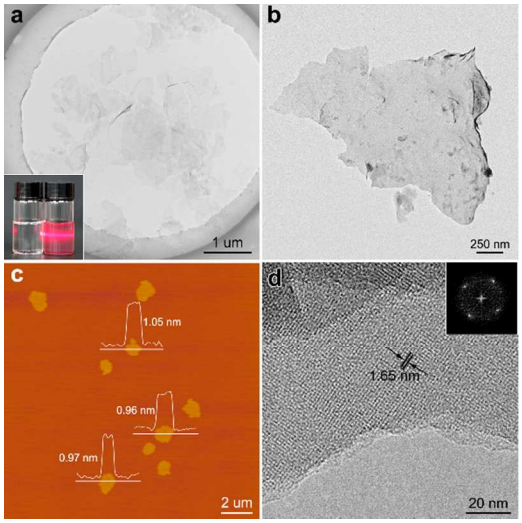

Figure 4. (a) TEM image of the exfoliated MOF nanosheets. Insert: Tyndall effect before (left) and after (right) exfoliation. (b) TEM image of an individual exfoliated MOF nanosheet. (c) AFM image of the exfoliated MOF nanosheets with corresponding height profiles. (d)

High-resolution TEM image of an exfoliated multilayer MOF nanosheet with the corresponding FFT pattern.

electron microscopy (TEM) and atomic force microscopy (AFM), respectively (Figure 4). Both characterization methods indicated that freestanding nanosheets with sizes up to micrometers were obtained after exfoliation (Figure S16a). Wrinkled or ruptured sheets can be observed from TEM (Figure 4a and 4b), suggesting ultrathin nature of the exfoliated nanosheets. As shown in Figure 4c and S16b, the height of as-exfoliated nanosheets is measured to ~1.0 nm with slight variations, roughly corresponding to the thickness of single-layer PdTCPP nanosheets (Figure S12).

The reduction of disulfide bonds is a chemical reaction which can be quantitatively controlled by varying the amount of TMP used along with the reaction time. Generally, in order to exfoliate MOF crystals into 2D nanosheets as much as possible, excess TMP is required. However, if the reaction time was shortened to 4 h and the amount of TMP used was 10-fold higher than that of the disulfide groups present in the crystals, the majority of obtained products were multilayer nanosheets with ~4 nm in height (Figure S17), indicating a controllable exfoliation process. More importantly, high-resolution TEM (HRTEM) clearly shows the lattice fringes of the exfoliated multilayer MOF nanosheets with an interplanar distance of 1.65 nm, which belongs to the (100) plane of intercalated crystals (Table S1). Meanwhile, the corresponding fast Fourier transform (FFT) image also displays a fourfold symmetry (Figure 4d). These results directly prove that the crystalline structure is still maintained after exfoliation. Thus, our results show that cleavage of DPDS could efficiently lead to the formation of ultrathin MOF nanosheets from intercalated MOFs. Control experiments by adding TMP or 4-mercaptopyridine to the Zn_2(PdTCPP) crystals could not lead to the spontaneous exfoliation process (Figure S18), confirming exfoliation starts with the reduction of DPDS ligands. The exfoliation is likely caused by the significantly decreased interlayer interactions after removing part of the intercalating agents, an extraction process similar to the synthesis of MXenes.[6d]

Recently, Zhang group reported a novel surfactant-assisted synthetic method to prepare ultrathin 2D MOF nanosheets with high yields.[2e] This method can conveniently produce multilayer nanosheets (<10 nm) but is difficult to achieve single-layer nanosheets. Moreover, liquid exfoliation method was used to exfoliate layered Zn_2(PdTCPP) crystals for comparison. Although irregular nanosheets with thickness in the range of 1.5~3.5 nm can be obtained, the majority of nanosheets are 30~120 nm in height (Figure S19 and S20). More importantly, the overall yield is ~10% with a large portion of small fragmented pieces (Figure S20). Therefore, selective chemical exfoliation from predesigned MOFs potentially allows for efficient and controllable formation of 2D MOF nanosheets.

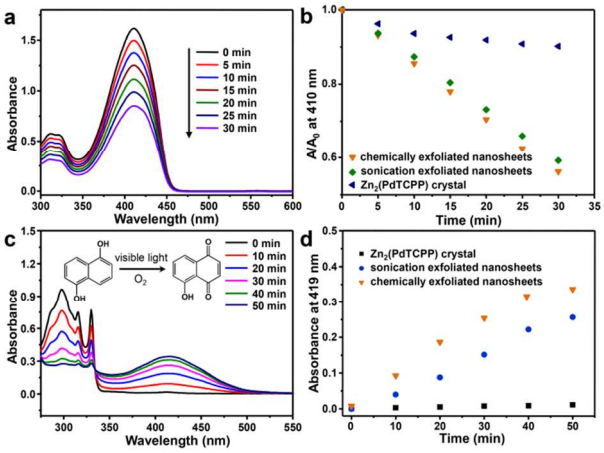

Figure 5. (a) UV-Vis absorption spectra of DPBF in the presence of chemically exfoliated MOF nanosheets upon visible light irradiation. (b) Absorbance decay of DPBF by different catalysts. (c) Photooxidation of DHN in CH_3CN catalyzed by chemically exfoliated nanosheets. (d) Absorbance of juglone (λ=419 nm) as a function of reaction time by different catalysts.

Ultrathin 2D nanosheets typically exhibit superior photoresponsivity and enhanced photocatalytic activity with more easily accessible reaction sites.[10] Porphyrin derivatives are widely used for $^1O_2$ generation due to their unique photochemistry and high-efficiency in light harvesting.[7c,11] We then further investigated the potential application of as-exfoliated nanosheets in $^1O_2$ generation for heterogeneous photocatalysis. 1, 3-diphenylisobenzofuran (DPBF) was used to detect the $^1O_2$ evolution upon visible light irradiation (λ>420 nm). As shown in Figure 5a, the absorption at 410 nm decreases in the presence of exfoliated MOF nanosheets, indicating the formation of $^1O_2$. The chemically exfoliated nanosheets exhibit better performance in $^1O_2$ generation compared to other samples (Figure 5b). As a result, the chemically exfoliated 2D MOF nanosheets are more efficient in photooxidation of 1,5-dihydroxynaphthalene (DHN) to form the corresponding oxidized product juglone (Figure 5c and 5d).

In conclusion, we have successfully demonstrated a versatile approach for synthesizing 2D MOF nanosheets with high yields. This novel strategy relies on the incorporation of a chemically scissable intercalating agent, 4, 4'-dipyridyl disulfide, into the intrinsically layered MOF crystals. The cleavage of intercalated disulfide groups occurs rapidly and, to a certain degree, is capable of controlling the thickness of exfoliated MOF nanosheets. Considering the vastly available organic ligands and metal nodes in MOFs, the approach demonstrated here holds great promise for synthesizing various ultrathin 2D metal-organic nanosheets with desired structures and properties.

ASSOCIATED CONTENT

Supporting Information

The Supporting Information is available free of charge on the ACS Publications website.

Detailed synthesis, single-crystal data, additional PXRD, SEM, TEM, AFM, NMR, and XPS characterization results.

AUTHOR INFORMATION

Corresponding Authors

hxu@ustc.edu.cn (H. X.); jianglab@ustc.edu.cn (H. L. J.); zhou@chem.tamu.edu (H. C. Z.)

Notes

The authors declare no competing financial interests.

ACKNOWLEDGMENT

We acknowledge 15U1 beamline at Shanghai Synchrotron Radiation Facility (SSRF) for the XRD measurements. We also thank Prof. S. Wang for acquiring the single crystal X-ray diffraction data. This work was supported by the National Key Basic Research Program of China (2015CB351903, 2014CB931803), the National Natural Science Foundation of China (51402282, 21474095, 21371162, 21673213 and 21521001), CAS Key Research Program of Frontier Sciences (QYZDB-SSW-SLH018). Y.-P. C was funded by Texas A&M University. H.-C. Z. gratefully acknowledges support from the Welch Foundation (A-0030).

REFERENCES

(1) (a) Novoselov, K. S.; Fal'ko, V. I.; Colombo, L.; Gellert, P. R.; Schwab, M. G.; Kim, K. *Nature* **2012**, *490*, 192. (b) Lv, R.; Robinson, J. A.; Schaak, R. E.; Sun, D.; Sun, Y.; Mallouk, T. E.; Terrones, M. *Acc. Chem. Res.* **2015**, *48*, 56. (c) Zhang, H. *ACS Nano* **2015**, *9*, 9451. (d) Wang, H.; Yuan, H.; Sae Hong, S.; Li, Y.; Cui, Y. *Chem. Soc. Rev.* **2015**, *44*, 2664.

(2) (a) Campbell, M. G.; Liu, S. F.; Swager, T. M.; Dincă, M. *J. Am. Chem. Soc.* **2015**, *137*, 13780. (b) Cao, L.; Lin, Z.; Peng, F.; Wang, W.; Huang, R.; Wang, C.; Yan, J.; Liang, J.; Zhang, Z.; Zhang, T.; Long, L.; Sun, J.; Lin, W. *Angew. Chem. Int. Ed.* **2016**, *55*, 4962. (c) Peng, Y.; Li, Y.; Ban, Y.; Jin, H.; Jiao, W.; Liu, X.; Yang, W. *Science* **2014**, *346*, 1356. (d) Rodenas, T.; Luz, I.; Prieto, G.; Seoane, B.; Miro, H.; Corma, A.; Kapteijn, F.; Llabres i Xamena, F. X.; Gascon, J. *Nat. Mater.* **2015**, *14*, 48. (e) Zhao, M.; Wang, Y.; Ma, Q.; Huang, Y.; Zhang, X.; Ping, J.; Zhang, Z.; Lu, Q.; Yu, Y.; Xu, H.; Zhao, Y.; Zhang, H. *Adv. Mater.* **2015**, *27*, 7372.

(3) (a) Makiura, R.; Motoyama, S.; Umemura, Y.; Yamanaka, H.; Sakata, O.; Kitagawa, H. *Nat. Mater.* **2010**, *9*, 565. (b) Tan, J. C.; Saines, P. J.; Bithell, E. G.; Cheetham, A. K. *ACS Nano* **2012**, *6*, 615. (c) Zhao, M.; Lu, Q.; Ma, Q.; Zhang, H. *Small Methods*, 2017, *1*, 201600030.

(4) (a) Naguib, M.; Gogotsi, Y. *Acc. Chem. Res.* **2015**, *48*, 128. (b) Niu, L.; Coleman, J. N.; Zhang, H.; Shin, H.; Chhowalla, M.; Zheng, Z. *Small* **2016**, *12*, 272. (c) Park, S.; Ruoff, R. S. *Nat. Nanotechnol.* **2009**, *4*, 217.

(5) (a) Cao, F.; Zhao, M.; Yu, Y.; Chen, B.; Huang, Y.; Yang, J.; Cao, X.; Lu, Q.; Zhang, X.; Zhang, Z.; Tan, C.; Zhang, H. *J. Am. Chem. Soc.* **2016**, *138*, 6924. (b) Hermosa, C.; Horrocks, B. R.; Martínez, J. I.; Liscio, F.; Gómez-Herrero, J.; Zamora, F. *Chem. Sci.* **2015**, *6*, 2553. (c) Foster, J. A.; Henke, S.; Schneemann, A.; Fischer, R. A.; Cheetham, A. K. *Chem. Commun.* **2016**, *52*, 10474. (d) Junggeburth, S. C.; Diehl, L.; Werner, S.; Duppel, V.; Sigle, W.; Lotsch, B. V. *J. Am. Chem. Soc.* **2013**, *135*, 6157. (e) Gallego, A.; Hermosa, C.; Castillo, O.; Berlanga, I.; Gomez-Garcia, C. J.; Mateo-Marti, E.; Martinez, J. I.; Flores, F.; Gomez-Navarro, C.; Gomez-Herrero, J.; Delgado, S.; Zamora, F. *Adv. Mater.* **2013**, *25*, 2141. (f) Li, P. Z.; Maeda, Y.; Xu, Q. *Chem. Commun.* **2011**, *47*, 8436. (g) Zhao, S. L.; Wang, Y; Dong, J. C; He, C. T; Yin, H. J; An, P. F; Zhao, K; Zhang, X. F; Gao, C; Zhang, L. J; Lv, J. W; Wang, J. X; Zhang, J. Q; Khattak, A. M; Khan, N. A; Wei, Z. X; Zhang, J; Liu, S. Q; Zhao, H. J; Tang, Z. Y. *Nat. Energy*, **2016**, *1*, 16184.

(6) (a) Zheng, J.; Zhang, H.; Dong, S.; Liu, Y.; Nai, C. T.; Shin, H. S.; Jeong, H. Y.; Liu, B.; Loh, K. P. *Nat. Commun.* **2014**, *5*, 2995. (b) Huang, X.; Zeng, Z.; Zhang, H. *Chem. Soc. Rev.* **2013**, *42*, 1934. (c) Ma, R.; Sasaki, T. *Acc. Chem. Res.* **2015**, *48*, 136. (d) Naguib, M.; Gogotsi, Y. *Acc. Chem. Res.* **2015**, *48*, 128.

(7) (a) Gao, W. Y.; Chrzanowski, M.; Ma, S. *Chem. Soc. Rev.* **2014**, *43*, 5841. (b) Morris, W.; Volosskiy, B.; Demir, S.; Gandara, F.; McGrier, P. L.; Furukawa, H.; Cascio, D.; Stoddart, J. F.; Yaghi, O. M. *Inorg. Chem.* **2012**, *51*, 6443. (c) Son, H. J.; Jin, S.; Patwardhan, S.; Wezenberg, S. J.; Jeong, N. C.; So, M.; Wilmer, C. E.; Sarjeant, A. A.; Schatz, G. C.; Snurr, R. Q.; Farha, O. K.; Wiederrecht, G. P.; Hupp, J. T. *J. Am. Chem. Soc.* **2013**, *135*, 862. (d) Park, J.; Feng, D.; Yuan, S.; Zhou, H. C. *Angew. Chem. Int. Ed.* **2015**, *54*, 430.

(8) (a) Burnett, B. J.; Choe, W. *CrystEngComm* **2012**, *14*, 6129. (b) Burnett, B. J.; Barron, P. M.; Hu, C.; Choe, W. *J. Am. Chem. Soc.* **2011**, *133*, 9984. (c) Karagiaridi, O.; Bury, W.; Mondloch, J. E.; Hupp, J. T.; Farha, O. K. *Angew. Chem. Int. Ed.* **2014**, *53*, 4530. (d) Li, T.; Kozlowski, M. T.; Doud, E. A.; Blakely, M. N.; Rosi, N. L. *J. Am. Chem. Soc.* **2013**, *135*, 11688.

(9) Choi, E. Y.; Barron, P. M.; Novotny, R. W.; Son, H. T; Hu, C. H; Choe, W. *Inorg. Chem.*, **2009,** *48*, 426.

(10) (a) Wang, H.; Yang, X.; Shao, W.; Chen, S.; Xie, J.; Zhang, X.; Wang, J.; Xie, Y. *J. Am. Chem. Soc.* **2015**, *137*, 11376. (b) Yang, S.; Gong, Y.; Zhang, J.; Zhan, L.; Ma, L.; Fang, Z.; Vajtai, R.; Wang, X.; Ajayan, P. M. *Adv. Mater.* **2013**, *25*, 2452.

(11) (a) DeRosa, M. C.; Crutchley, R. J. *Coord. Chem. Rev.* **2002**, *233-234*, 351. (b) Chen, Y. Z.; Wang, Z. U.; Wang, H.; Lu, J.; Yu, S. H.; Jiang, H. L. *J. Am. Chem. Soc.* **2017**, *139*, 2035.

Table of Contents (TOC)

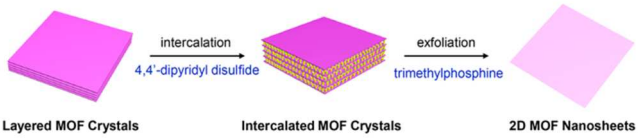
intercalation
4,4'-dipyridyl disulfide
exfoliation
trimethylphosphine
Layered MOF Crystals
Intercalated MOF Crystals
2D MOF Nanosheets